ULTRASTRUCTURAL CHARACTERISTICS OF WOOD FRACTURE SURFACES

W. A. Côté and *R. B. Hanna*

Professor and Director, and Associate Professor and Assistant Director, respectively
N. C. Brown Center for Ultrastructure Studies, State University of New York
College of Environmental Science and Forestry
Syracuse, NY 13120

(Received 8 April 1982)

ABSTRACT

This study concentrated on the ultrastructural characteristics of hardwood fracture surfaces, but it included southern yellow pine as a representative softwood for comparison. Very small specimens were made, tested for compression parallel to the grain, tension parallel to the grain, shear in the radial plane and shear in the tangential plane, and were then prepared for scanning electron microscopy. Secondary electron micrographs of the fracture zones were recorded singly or in stereo pairs, and a number are used to illustrate the major findings.

Thick-wall cells tend to fail in an intrawall pattern at the S1/S2 interface, while thin-walled cells are more likely to fail with transwall fracture. In tangential shear tests of ring-porous woods, the plane of fracture follows the earlywood vessels which are thin-walled and have wide lumens. Large oak-type rays affect the fracture path in all of the test modes. Certain characteristic types of failure can be related to each of the testing modes utilized.

Keywords: Scanning electron microscopy, compression parallel to the grain, tension parallel to the grain, radial shear, tangential shear, intrawall failure, transwall failure, intercell failure, fracture paths, fracture surface.

INTRODUCTION

During the many decades in which the mechanical testing of wood has been practiced, characteristic patterns of gross- or macro-failure in standard test specimens have become well recognized and generally predictable. These tests have included compression parallel to the grain, tension parallel to the grain, radial shear, and tangential shear. Relatively recently, interest has developed in the nature of wood fracture at the microscopic and even at the ultrastructural level. No doubt the more general availability and increased use of scanning electron microscopy (SEM) have been major factors in this trend. However, realization of the importance of the morphological influence on the nature of fracture in wood is not as new as scanning electron microscopy.

A few examples of the appreciation of anatomical considerations in wood behavior can be cited. Clarke (1935) related structure to failure of ash wood using light microscopic evidence. In 1951, Wardrop published the results of a study in which the microstructure of coniferous tracheids was related to the breaking load in tension of specimens microtomed to 80 micrometers in thickness. This approach permitted comparison of specimens from earlywood and latewood of one growth increment, or of successive growth rings. Details of the technique were reported by Kloot in 1952.

Tiemann (1951) in his reference work on wood technology included anatomical relationships to mechanical failure. In 1963, Kollmann described the phenomena of fracture in wood and used photomicrographs to illustrate microscopic defor-

Wood and Fiber Science, 15(2), 1983, pp. 135–163

mations and cracks. He also wrote about submicroscopic "slips" which other authors had theorized about earlier in the century.

Wardrop and Addo-Ashong (1965) prepared an extensive review of the anatomy and the "molecular and supermolecular" organization of wood as background for a clearer understanding of structural changes related to mechanical failure. A number of light and transmission electron micrographs illustrated the structural deformation and failure at the cell-wall level resulting from tests in compression and tension parallel to the grain.

Pentoney with coworkers DeBaise and Porter (1966) explored the morphology and mechanics of wood fracture. They were particularly concerned with crack propagation in wood shear fracture. DeBaise (1970, 1972) was one of the first to examine cell-wall layers following failure to determine the precise location of fracture. The scanning electron microscope was employed in this research. He found that slow crack propagation produced relatively smooth fracture surfaces, while rougher surfaces resulted from rapid crack propagation. He also introduced the terms "intercellular" and "intracellular fracture" to describe the nature and location of failure between and within coniferous wood cells.

The importance of wood failure in mechanical pulping was investigated by a number of individuals, but Koran (1967) utilized both scanning electron microscopy and transmission electron microscopy in his studies on black spruce. The radial and tangential surfaces of this material generated through tensile failure at various temperatures were examined in detail and analyzed critically. He introduced "trans-wall failure" and "intra-wall failure" into the terminology on fracture. Woodward (1980) used green ponderosa pine to evaluate the effect of elevated temperatures on its tensile behavior and fracture path orientation as related to location of hemicelluloses in the cell wall.

In the present study, emphasis was placed on fracture modes in hardwoods because of the apparent lack of published information in this area. In addition, the specimens were prepared from wood samples taken from small trees, less than 6 inches in diameter, and grown on southern pine sites—i.e., on poor hardwood sites.

The types of tests included in this research were compression parallel to the grain, tension parallel to the grain, shear in the radial plane, and shear in the tangential plane. For comparison, a representative softwood, southern yellow pine, was included with the three hardwood species selected. The same specimen sizes and testing procedures were employed for both softwoods and hardwoods.

MATERIALS AND METHODS

Since many of the hardwood trees grown on southern pine sites are small in diameter (less than 6 inches), large standard-size test specimens cannot always be readily produced. For this study only small size wood samples could be provided by the Pineville Laboratory at the time the study was being initiated. To assure having authenticated material, as well as for other reasons outlined below, it was decided to scale down test specimen size to fit the available wood samples.

This approach is recommended by ASTM Standard D143-52 for such circumstances. However, even under the recommended ASTM "Secondary methods," only specimens for compression parallel to the grain tests are reduced in size; in

this case the reduction is from 5 × 5 × 20 cm to 2.5 × 2.5 × 10 cm. All of the other mechanical tests are to be conducted with 5-cm × 5-cm cross-section material with length adjusted to the nature of the specific test. Unfortunately, even the reduced size indicated for compression parallel to the grain was too large for the available material. Therefore much smaller sizes were utilized as discussed under "Specimen preparation."

Another very practical reason for utilizing small test specimens is related to the type of microscopy employed for the study. The scanning electron microscope requires that the specimen be relatively small if high vacuum is to be achieved within a reasonable time. Also, the chamber size will not accommodate entire specimens of standard size. They must be cut, and cutting artifacts may be created in this process since mechanical damage is difficult to avoid in sawing or machining.

When large specimens are tested to failure, it is sometimes difficult to locate a characteristic failure zone. By using small samples, the failure zone is readily located and further cutting is eliminated or minimized. In tensile test specimens the failure can be concentrated in a necked-down region only 2 × 3 mm in cross-section, for example. In shear tests specimens, an entire failure zone can be concentrated either in the earlywood or in the latewood thus offering ideal opportunities for observing the differences in behavior in the two regions.

It may be questioned whether very small samples behave in the same way as standard large samples in mechanical testing. From preliminary trials, it was found that, indeed, very small samples do fail in the characteristic gross pattern, provided that the test fixtures are appropriately designed and that correct proportions are maintained in the small specimens. Samples for compression parallel to the grain offer a good example of the similarity of behavior. Specimens only 1 cm in cross-section fail with the same well-defined buckling pattern as exhibited in ASTM standard size specimens. The line of buckling failure, as viewed on the tangential face, made an angle of 45 to 60 degrees with the grain or axial direction of the specimen. Round specimens, 1 cm in diameter, fail with a single line of buckling at approximately the same angle as in the square or rectangular cross-section samples.

Specimen preparation

Three hardwood species and one softwood were selected for the study. The hardwoods were chosen from the species grown on southern pine sites. Included were red oak, sweetgum and hickory. Diffuse- and ring-porous woods were represented in the selection. Southern pine, species undetermined, was chosen to represent the softwoods and as a comparison in ultrastructural interpretation.

The compression parallel to the grain test specimens were 1 cm in cross-section. They were cut 3 cm in length. The round cross-section specimens for the compression test were also 3 cm long and 1 cm in diameter.

For the shear tests, the specimens were 1 cm and 2.5 × 2.5 cm. The shear plane was oriented either tangentially or radially as required.

Samples for the tensile test, parallel to the grain, needed to be long enough to provide adequate gripping surface. Also, in order to provide a relatively long, straight-grained region in the necked-down portion, the overall length needed to

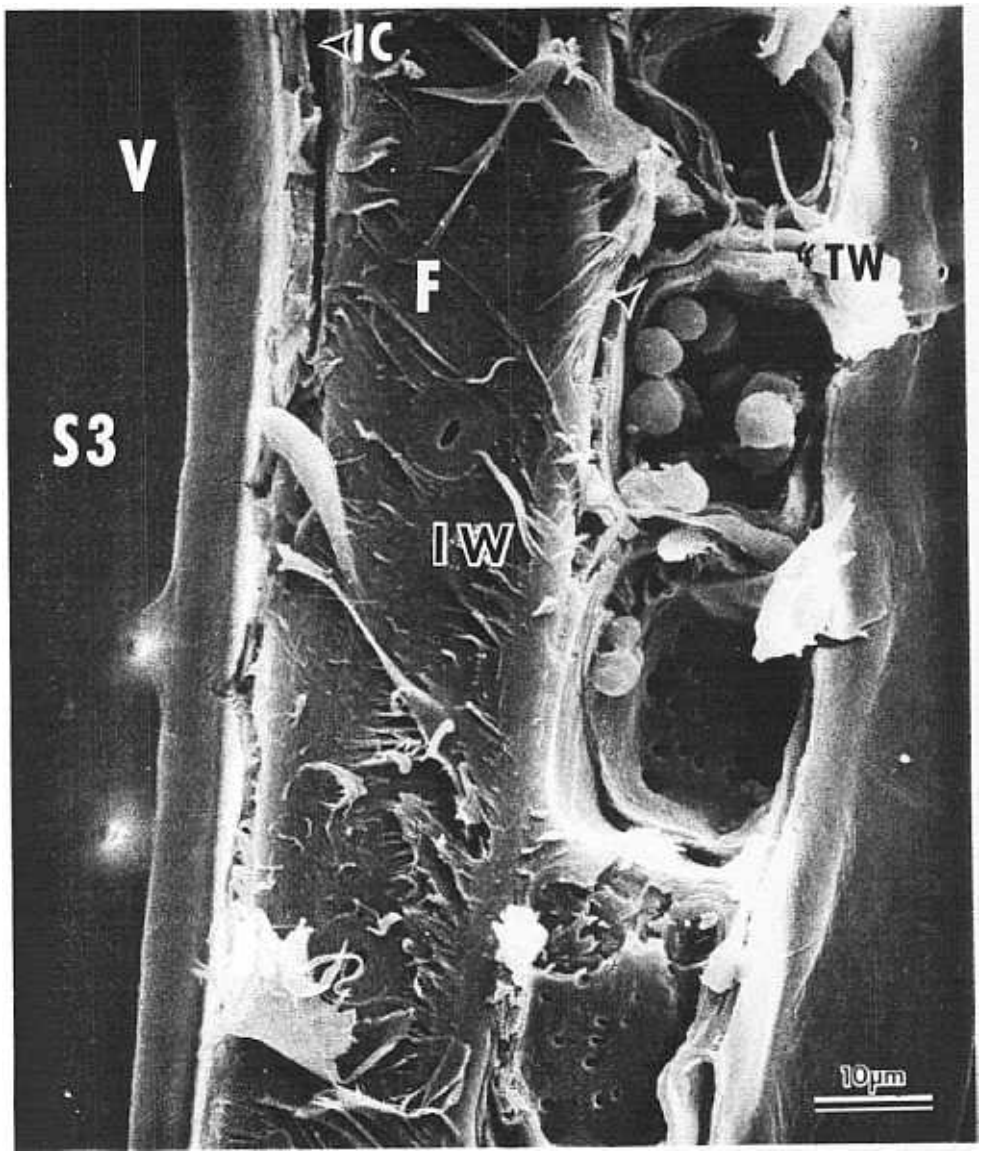

FIG. 1. In this micrograph of sweetgum that failed in tangential shear, both transwall (TW) and intrawall (IW) failure can be noted in adjoining cells. The ray parenchyma cell wall has delaminated (arrow). The lumen lining layers (S3) appear to be intact in cells at both right and left extreme edges of this micrograph. Intercell failure appears at upper center at the vessel and fiber interface.

Symbols used on figures.—F = Fiber; FL = Fiber lumen; IC = Intercell failure; IW = Intrawall failure; ML = Middle lamella; RP = Ray parenchyma; S1 = Outer layer of secondary wall; S2 = Middle layer of secondary wall; S3 = Inner layer of secondary wall; S1/S2 = Interface of S1 and S2; S2/S3 = Interface of S2 and S3; TW = Transwall failure; V = Vessel.

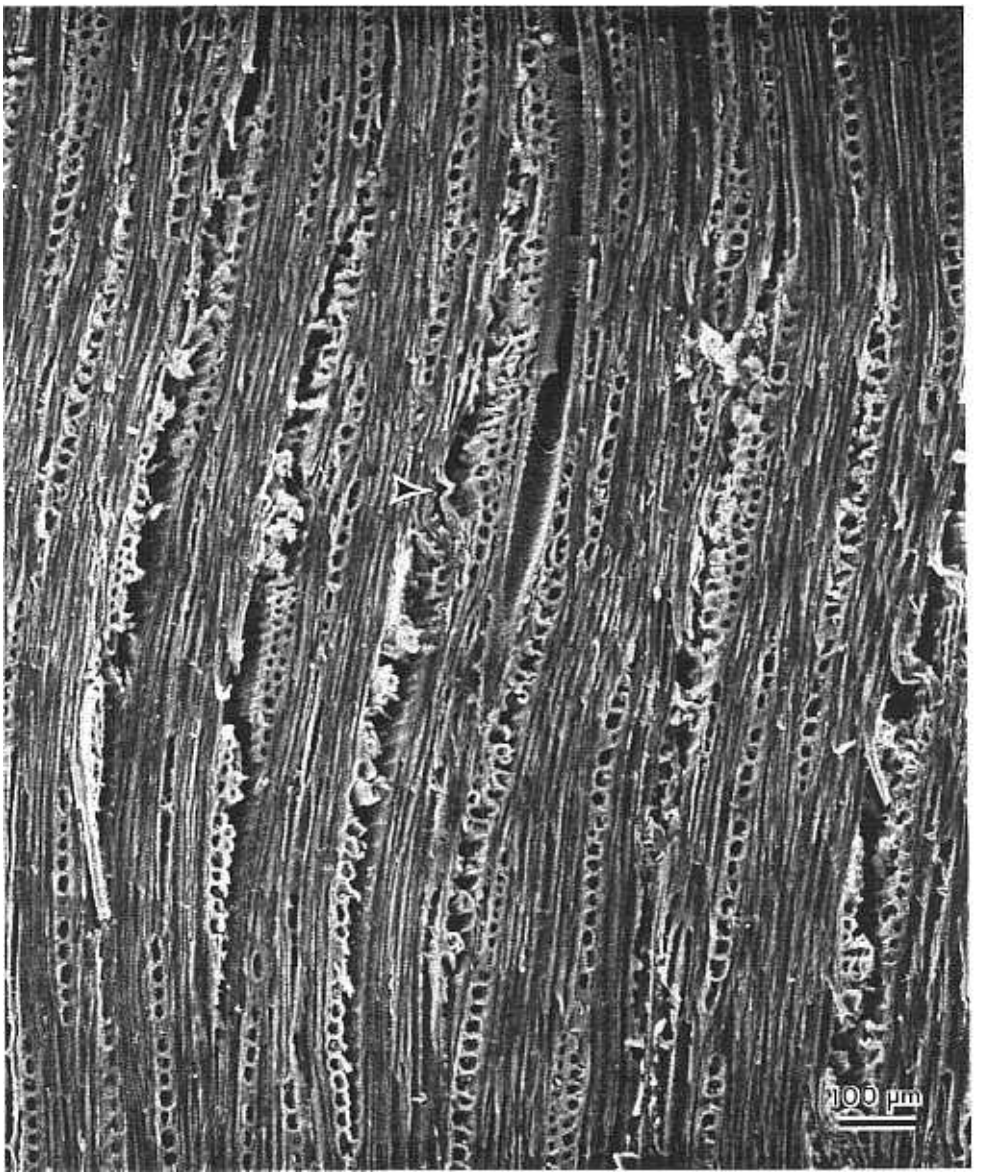

FIG. 2. Tangential surface of red oak compression test specimen showing the start of gross buckling and the initiation of separation in the vicinity of rays. Intercell failure proceeds above or below the rays, but appears to have started at fiber/ray interface in most cases. Arrow indicates area enlarged in Fig. 3.

be 15 cm. This provided a stress-concentration area 3 cm long and 2 × 3 cm in cross-section.

All of the samples were tested at the nominal moisture content of 8 to 10%. No attempt was made to build an environmental chamber around the test area of the testing machines. Although strength values were noted, testing to failure

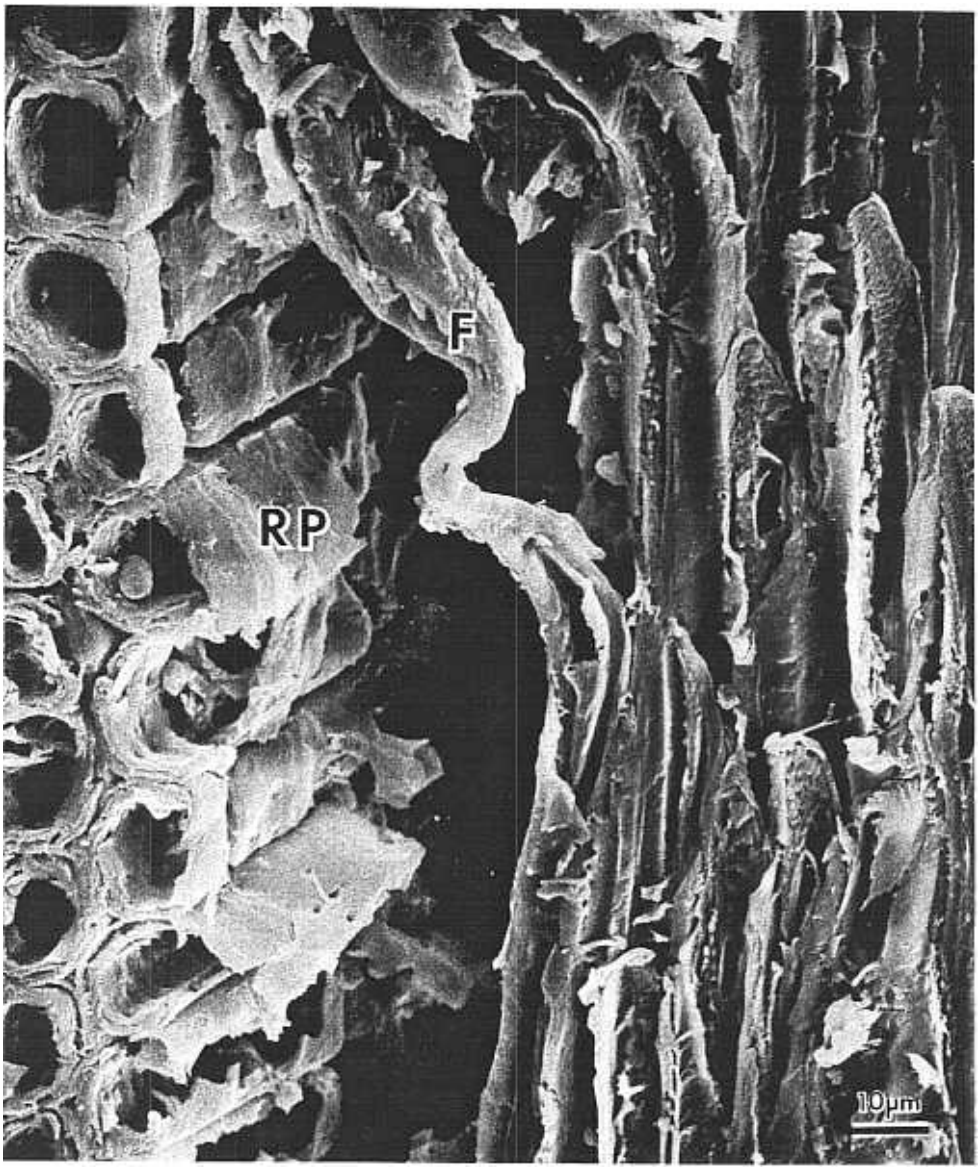

FIG. 3. Area indicated by arrow in Fig. 2 was recorded after inverting the compression test specimen and increasing the magnification approximately tenfold. The buckling of fibers and the separation of fibers from the ray parenchyma tissue in intercell failure are emphasized.

was purely qualitative with the objective of creating fracture surfaces for examination and analysis.

Microscopy

The scanning electron microscope was selected as the ideal instrument for this study. Specimens could be examined in some instances with no chance of mechanical damage or artifact production since the entire test specimen would fit into

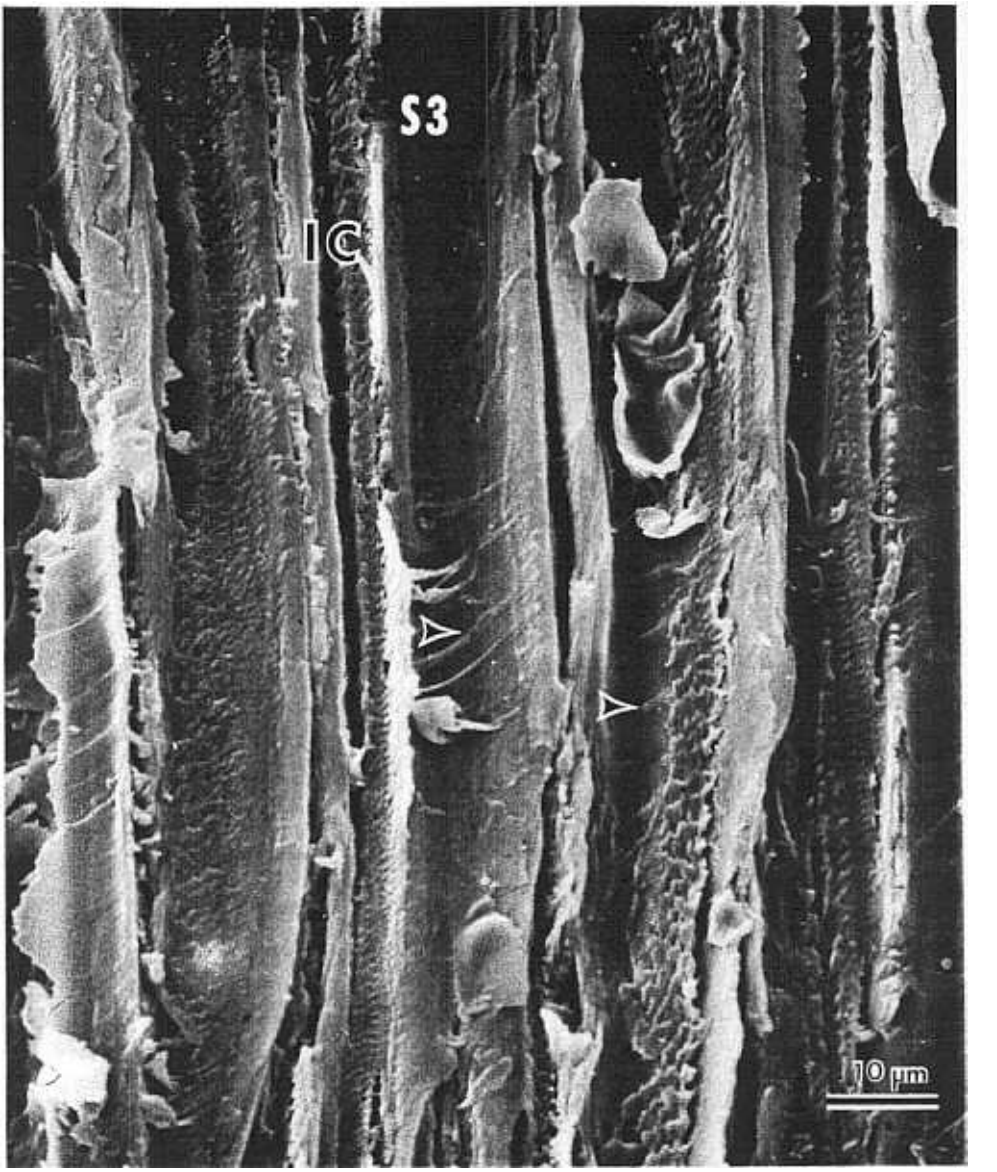

FIG. 4. Hickory compression specimen which exhibits cell-wall deformations visible in the cell lumens, separation of fibers at or near the middle lamella and intrawall failure. Arrows indicate S3 deformations.

the chamber. This was possible for shear test specimens and for the outer views of the compression test specimens. All of these could be attached to the specimen supports with adhesive and then sputter-coated with gold/palladium with but one intermediate step. All had to be oven-dried since they would be introduced into the high vacuum system of the scanning electron microscope.

For interior views of the compression test specimens, soaking in water, microtoming, then oven-drying and sputter coating were required. Both the round and

FIG. 5. Tangential view of a sweetgum specimen tested in compression parallel to the grain. The extreme buckling even at this microscopic level results from separation of cells above and below the buckling zone. Both intercell and intrawall failure can be seen in this micrograph.

the square cross-section specimens were so processed. Radial and tangential surfaces were produced by microtoming so that clear observations in both aspects would be possible.

The tensile test specimens were prepared by simply cutting off a 1- to 2-cm portion of the necked-down region, with the fracture zone left untouched at the end. The cut end was then attached to the specimen holder after oven-drying. Matching ends were mounted separately, but it proved to be impossible to find

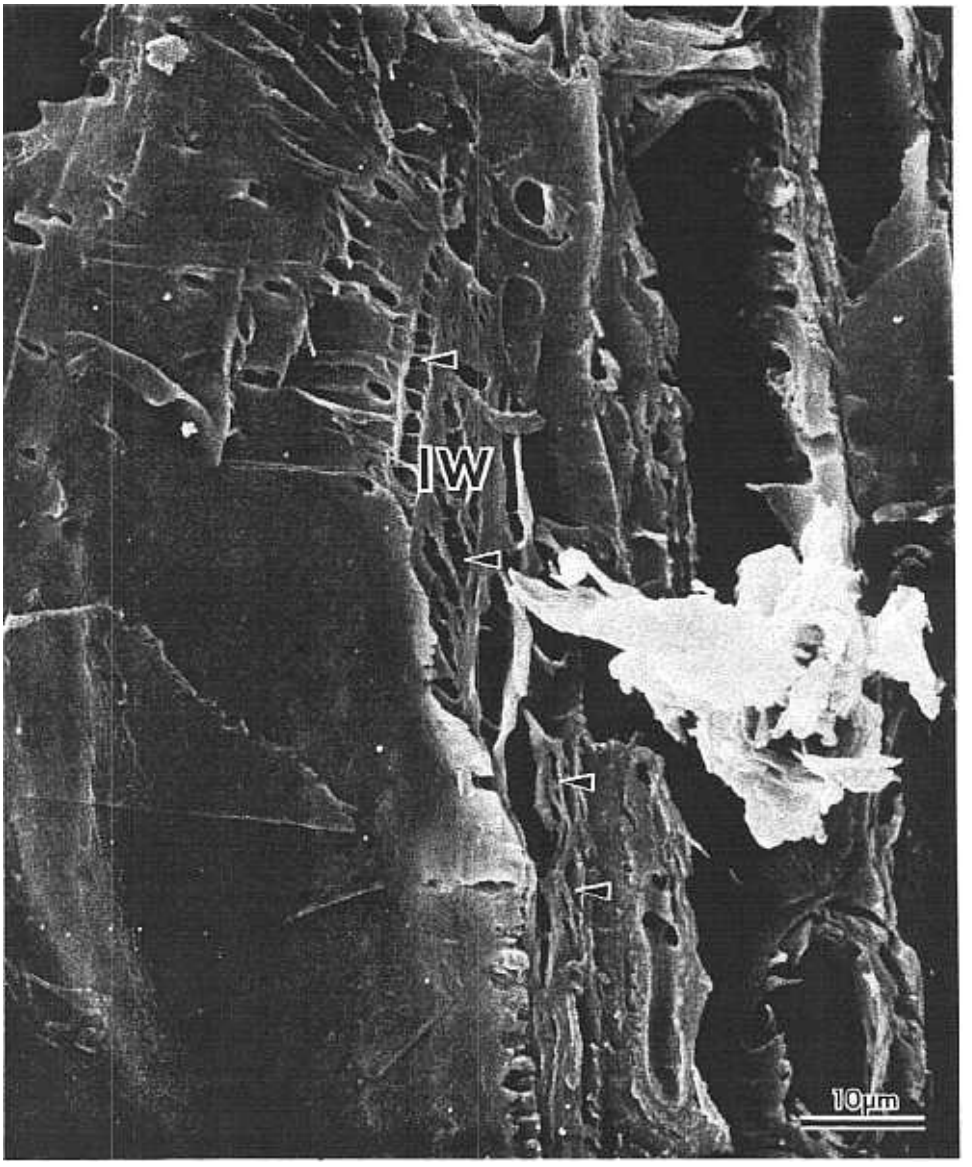

FIG. 6. This micrograph of red oak was selected to illustrate the initiation of buckling within the fiber wall (arrow) when tested in compression parallel to the grain. These early signs of intrawall failure may be detected in sections viewed with polarization microscopy.

matching anatomical structures in the SEM. Gold/palladium sputter coating was used for these specimens as well.

The instrument used for all of the scanning electron microscopy was the ETEC Autoscan. Secondary electron micrographs were recorded at magnifications of 60× to 1,700× on Polaroid Type 55 P/N film. The 4-inch × 5-inch negatives produced were then used for preparation of the enlargements illustrating this report.

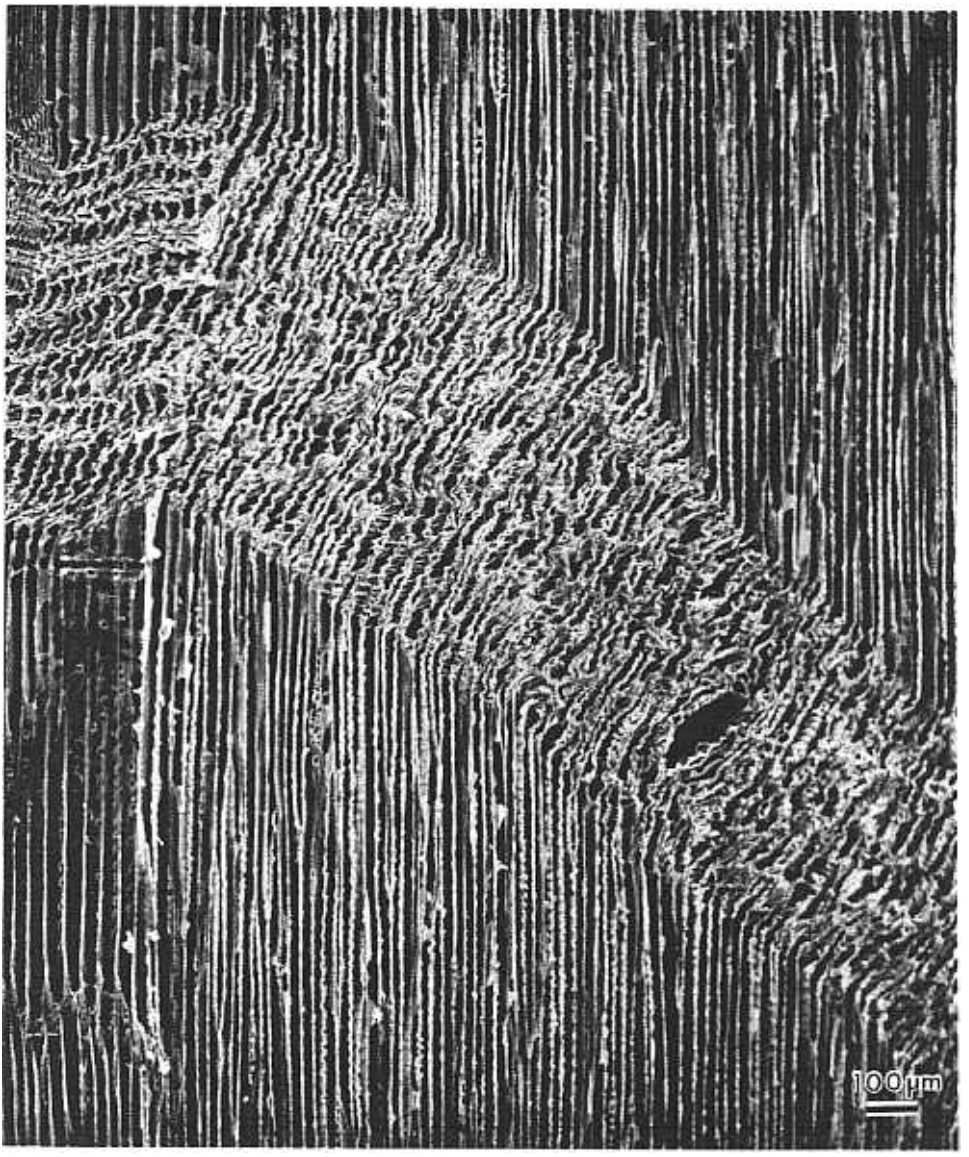

FIG. 7. The failure lines resulting from compression parallel to the grain are distinct in softwoods such as this sample of southern pine, which is mostly earlywood, because of the relatively simpler anatomical structure. The characteristic 45° to 60° angle made by the failure line with the axial direction of the wood is apparent even at this magnification.

To make the interpretation of the micrographs simpler and more accurate, stereo pairs were prepared in a number of cases and in each test category. In these instances one micrograph was recorded at −5° tilt, while the other was recorded at +5°. Although only a selected few micrographs in each category are included in this report, an extensive file of micrographs was prepared from which to make the selection.

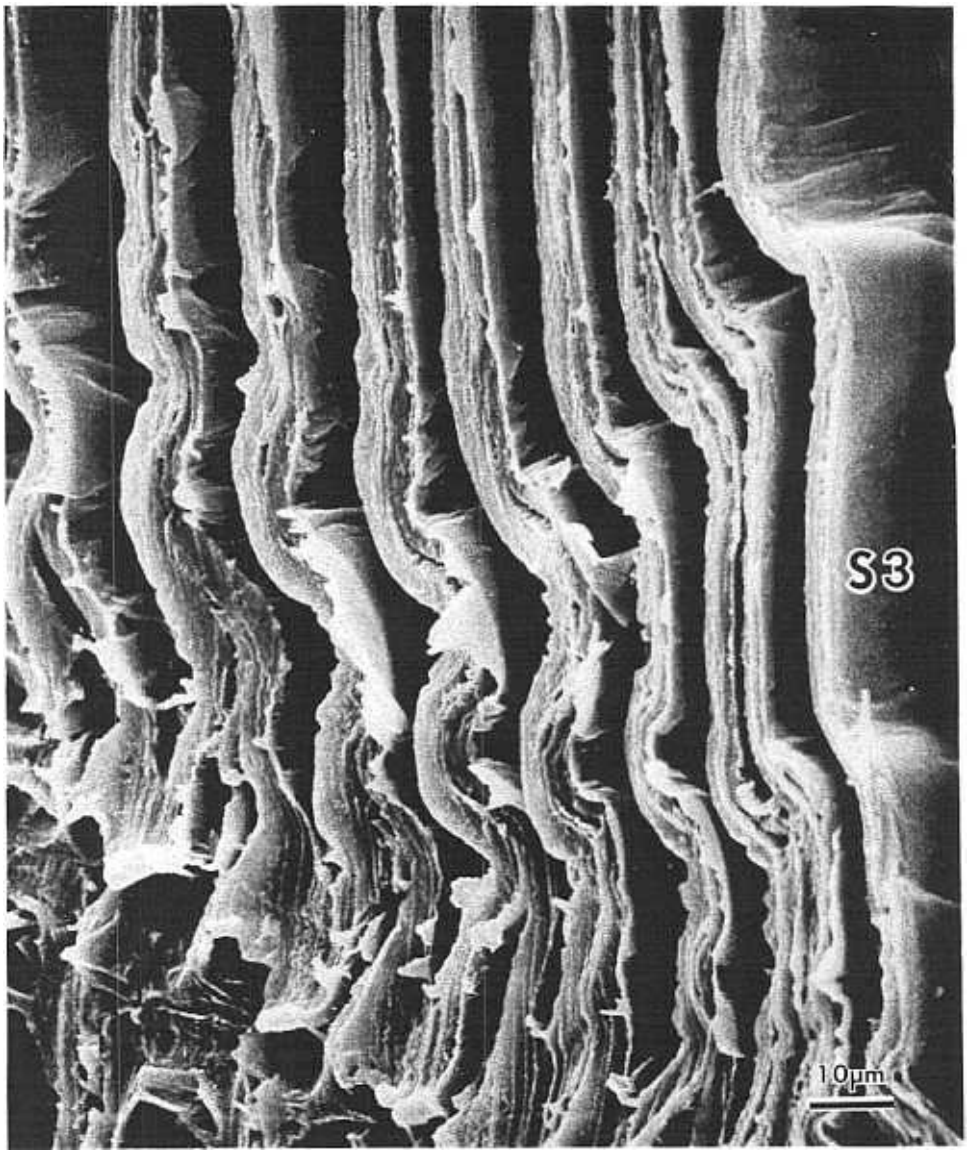

FIG. 8. When a limited area, latewood, of the sample shown in Fig. 7 is recorded at a higher magnification, the failure zone shows the typical buckling of the tracheid walls which results in distortion of the S3 and intercell failure.

RESULTS AND DISCUSSION

For purposes of discussion, we have grouped the results into three categories: compression parallel to the grain, shear parallel to the grain, and tension parallel to the grain. Both radial and tangential shear modes are included in the interpretation of the results of shear tests. The test results for the southern pine specimens are included for direct comparison within each category. To the extent possible, examples of each of the hardwood species have been included for each test mode.

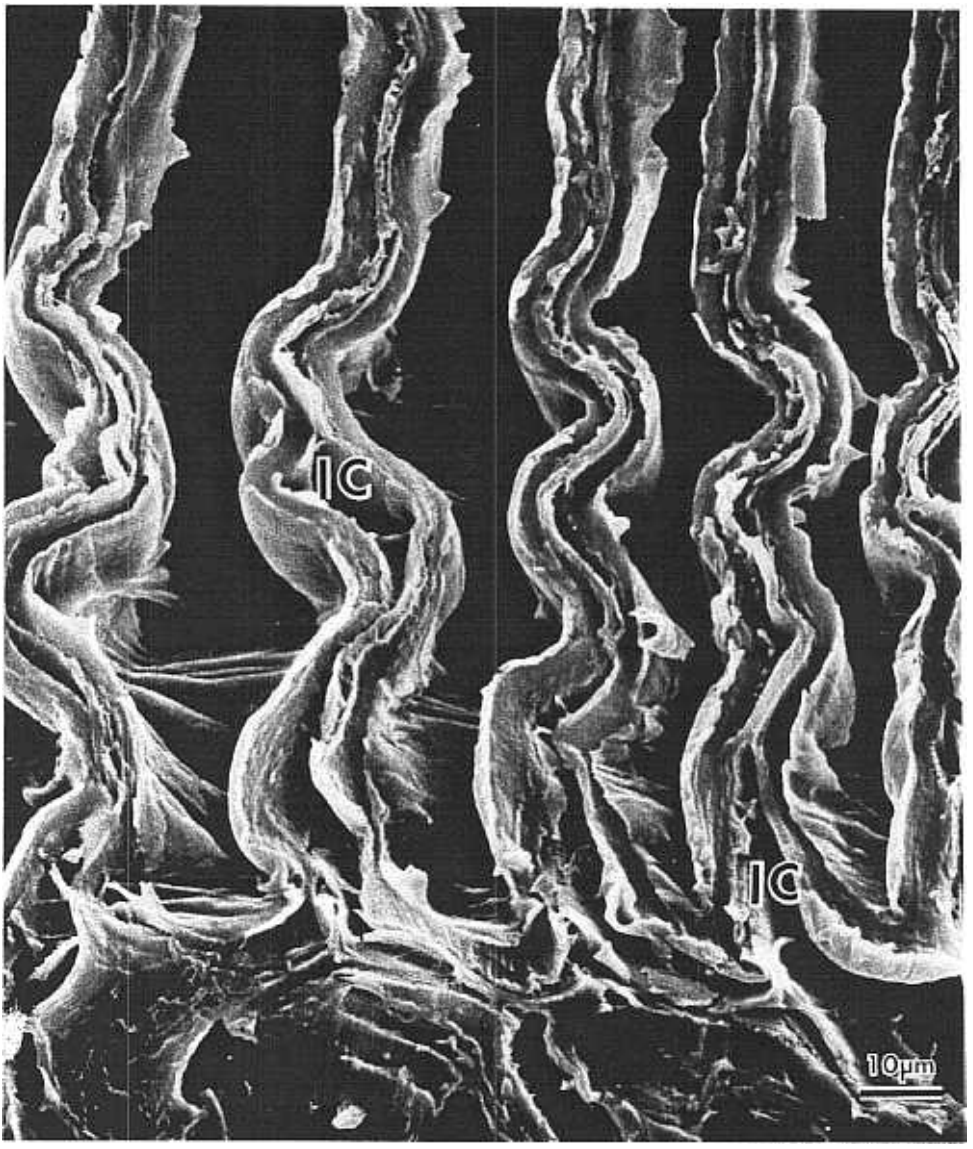

FIG. 9. Intercell failure in the buckling zone of a southern pine compression test specimen is more obvious when the microtomed surface is recorded with a minimum of tilt.

Terminology

Unless one is accustomed to dealing with wood structure at the sub-light microscopic level and using the specialized terminology that has developed in this area, it can be difficult to describe failure phenomena or to understand the descriptions. Most wood cell walls consist of three-layered structure in the secondary wall and an outer primary wall envelope, which is in contact with intercellular substance called the middle lamella. The secondary wall layers have been designated S1, S2, and S3 for convenience. These symbols refer to the outer, middle, and inner secondary wall layers, respectively.

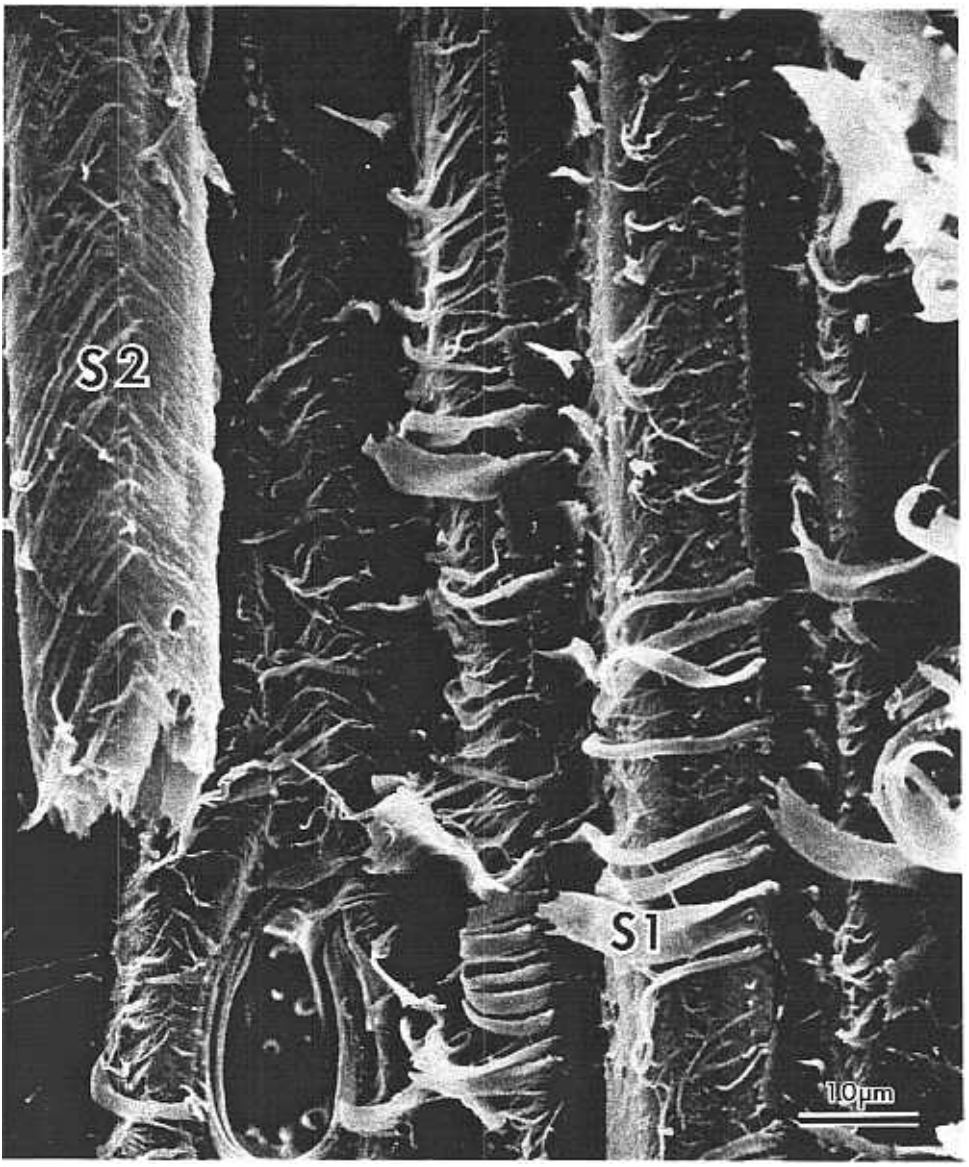

FIG. 10. Intrawall failure predominates in the thick-walled cells of this hickory specimen that failed in tangential shear. The S2 and the S1 are the more prominent layers visible in this micrograph. Intrawall failure takes place within either the S1 or the S2, or at their interface, the S1/S2. The single ray parenchyma cell, lower left, exhibits transwall fracture.

When failure occurs, three types of breaks can be recognized: intercell, intrawall, and transwall. *Intercell failure* occurs at the middle lamella and is simply the separation of cells at this junction. *Intrawall failure* refers to failure within the secondary wall and in most instances it is at the S1/S2 interface or close to it. When rupture of the wall is complete (when the fracture path cuts across the wall) the failure is described as *transwall.*

FIG. 11. A fracture surface very similar to that in Fig. 10 is produced in radial shear testing as in this red oak specimen. Intrawall failure of the longitudinal elements involves the S1 or the S2, or their mutual interface. This micrograph resembles that of Fig. 10 except that one fiber lumen was left intact (center), presumably because of transwall failure.

Figure 1 has been labeled to illustrate each of the above types of failure: IC refers to intercell failure, IW is intrawall failure, and TW is transwall failure. In this case the ray parenchyma cells were sheared off in transwall failure as was the double wall of the vessel (V) and the adjoining fiber (F). Intrawall failure took place within the fiber wall apparently at the S1/S2 interface.

FIG. 12. Sweetgum tested in tangential shear appears to fail primarily with transwall fracture, probably because of the reduced cell-wall strength when the S2 is thin. However, careful inspection of some of the cell lumens reveals a few instances of intrawall damage.

Compression parallel to the grain

Hardwoods loaded in compression parallel to the grain develop visibly well-defined patterns of buckling failures. On the tangential faces of failed specimens, the lines of failure make an angle of 45° to 60° to the axial (grain) direction (Fig. 2). The failure lines are the result of intercellular separation at the ray/fiber interface (Figs. 2, 3). Separation occurs at the middle lamella (Figs. 3, 4). However,

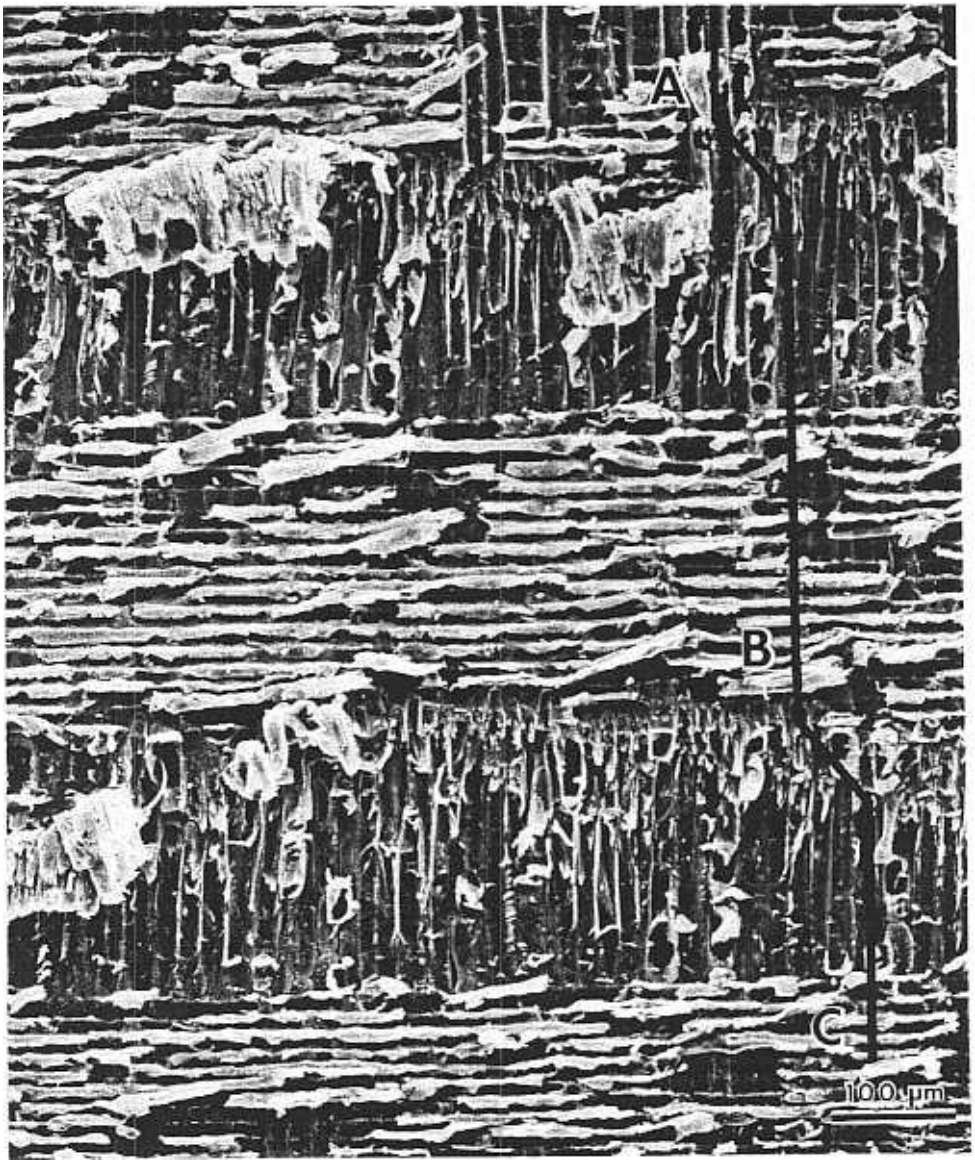

FIG. 13. The stepwise fracture path in radial shear specimens is evident in this micrograph. Failure apparently proceeded from Ray A to Ray B to Ray C as indicated by the open lumens immediately below each ray. Intrawall failure appears in nearly all of the parenchyma cells of this red oak specimen.

shear stresses also accompany these deformations and the resulting intrawall failures then occur between the S1 and S2 layers (Figs. 3, 5).

The macroscopic buckling of the fibers (Figs. 2, 5) is preceded by minute deformations of the cell wall (Figs. 4, 6). Figure 4 is a micrograph in which the intrawall deformations or slip planes (arrows) are easily seen. This type of failure was described and illustrated with photomicrographs by Keith and Côté (1968).

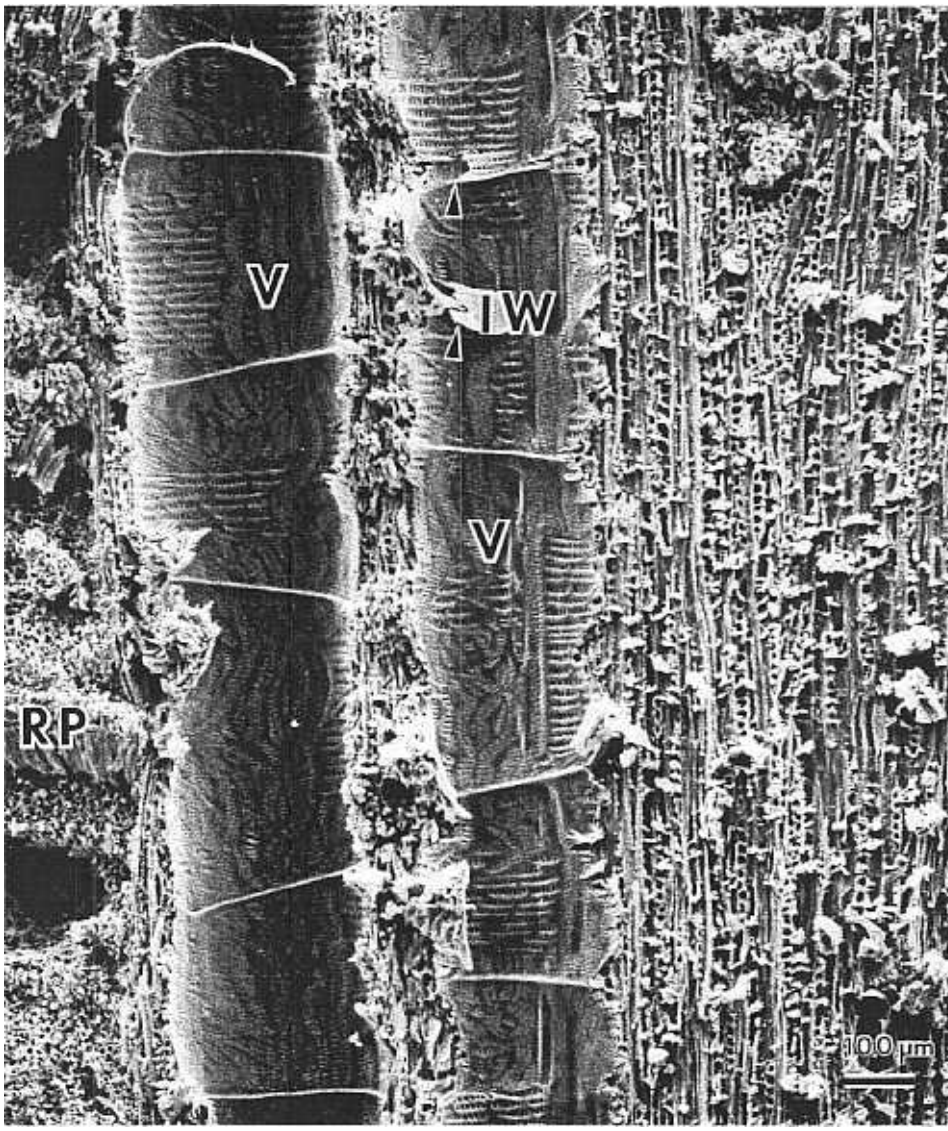

FIG. 14. In ring-porous woods, tangential shear tends to focus in the earlywood region where large, thin-walled vessels are concentrated. This is evidenced in this red oak specimen where transwall failure predominates in the rays as well as the vessels. Some intrawall failure does occur in the vessels (arrow), but the breaks are generally clean.

There did not appear to be any differences in failure between diffuse-porous and ring-porous hardwoods. The most prominent feature of failure in compression parallel to the grain was the separation at the ray/fiber interface.

Because of the relatively simpler anatomy of coniferous wood, the failure lines are more distinct than in hardwoods where a variety of cell types may tend to mask the deformations. At a low magnification such as in Fig. 7 the buckling failure in southern pine is particularly striking. The 45° to 60° angle the failure

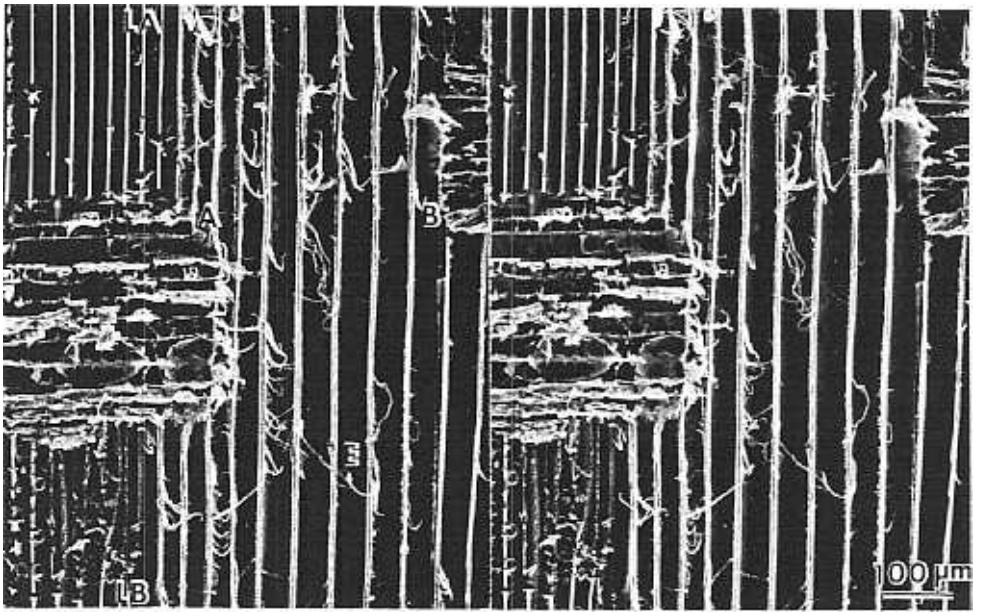

FIG. 15. Radial shear in southern pine, when viewed at low magnification, reinforces the concept of cell-wall thickness as the determining factor leading to intrawall vs. transwall failure. This stereo pair makes it easier to compare the fracture zones in earlywood (E) and latewood (LA and LB).

line makes with the axial direction of the wood is very clear as it is in Fig. 8, which was recorded at 700×. In the latter micrograph the "domino effect" of the buckling failure can be observed through the characteristically compressed or crimped cell walls.

At the same magnification, the compound cell walls (two adjoining tracheid walls with middle lamella) (Fig. 9) show little rupture, but there is considerable intercell failure. Microtoming was necessary to reveal the detail in the compression parallel to the grain specimens.

Shear parallel to the grain

When hardwoods are subjected to shear stresses parallel to the grain, there are similarities in the nature of the failure in the radial and tangential modes. In species of relatively high specific gravity, the microfibrils of the thick S2 cell-wall layer resist the shear stresses because of their orientation. Consequently, the intrawall failures occur at the S1/S2 interface in both modes of testing. For example, Fig. 10 is a hickory specimen tested in the tangential plane. Fragments of the S1 layer with more or less horizontal orientation are torn away from the S2, which exhibits fibrillar orientation of approximately 60° or 70° from the horizontal (20° or 30° from the axial). In Fig. 11, which is a red oak radial shear specimen, the fiber walls fail in much the same pattern.

In species with a lower specific gravity, the S2 layer is greatly reduced in thickness and therefore the failures tend to be transwall. Figure 12 is a specimen of sweetgum that failed in tangential shear, and the failures in this case are largely

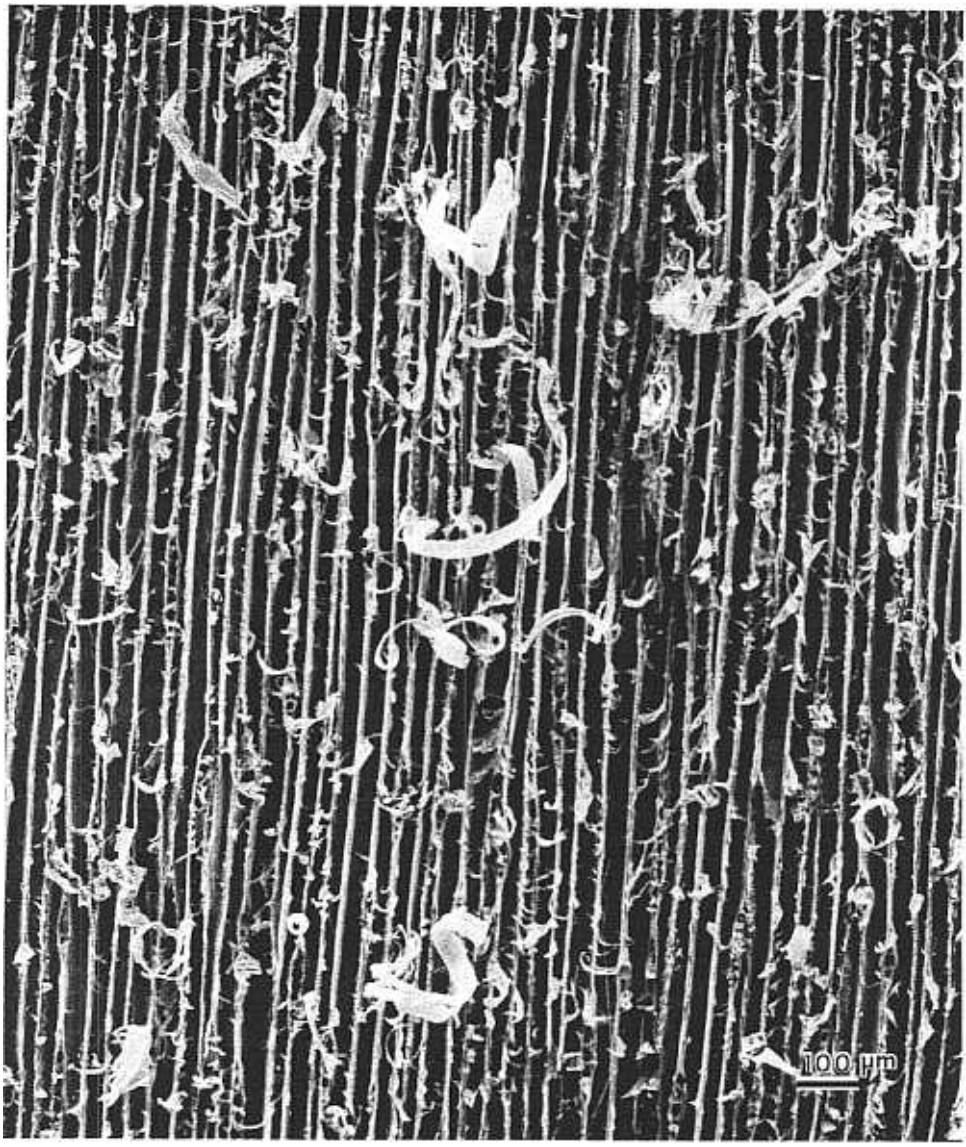

FIG. 16. When southern pine was subjected to tangential shear, the fracture zone was generally in the earlywood. The cell-wall failures were of the transwall type. In this micrograph there are a few "flags" of secondary wall, which peeled out of the tracheids. Evidently there was intrawall failure at the S1/S2, which resulted in S2/S3 layers pulling out of the fracture plane.

transwall since vessels predominate. Where there are fibers, intrawall failure can be observed.

When viewed at the macroscopic level, the fracture plane is also seen to pass through the areas of least resistance. In radial shear this zone of weakness is through the rays. In Fig. 13, radial shear in red oak, the fracture plane has proceeded in a steplike manner from the plane of ray A to the plane of ray B to the

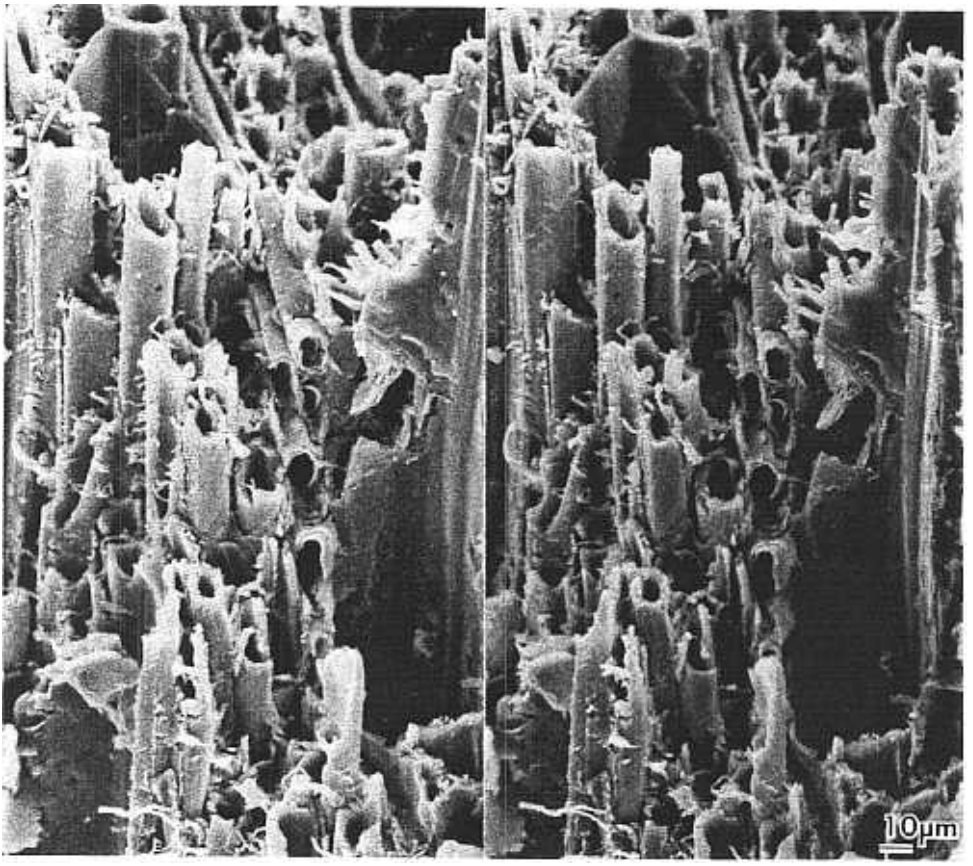

FIG. 17. If a relatively low specific gravity wood, such as sweetgum in this micrograph, is tested to failure in tension, transwall fractures predominate because of the thin cell walls. Some intrawall failure can be found in this stereo pair and, as in most other instances, it occurs at the S1/S2.

plane of ray C (broken line). Vessel elements did not appear to have any significant effect in radial shear because of the dominant weakness in the plane of the rays.

In tangential shear specimens, there is a distinct zone of weakness in the earlywood region of ring-porous hardwoods. Failure is transwall through the vessel elements (Fig. 14) and the ray cells, offering little shear resistance, pull out in pieces. The fibers show intrawall failure.

Southern yellow pine exhibits the same failure characteristics in shear parallel to the grain that was observed in the hardwoods. Figure 15 is a stereo pair selected to demonstrate more clearly the three-dimensional aspects of a fracture surface, in southern pine in this instance. In the earlywood region (E), there is transwall failure due to the diminished thickness of the S2 layer. In the latewood region there is intrawall failure at the S1/S2 interface. In the area (LA) above the ray A the residual S1 can be seen, while below ray B the S2 fracture surface appears in the equivalent of a complementary area.

As in the hardwoods, the rays determine the plane of failure in radial shear.

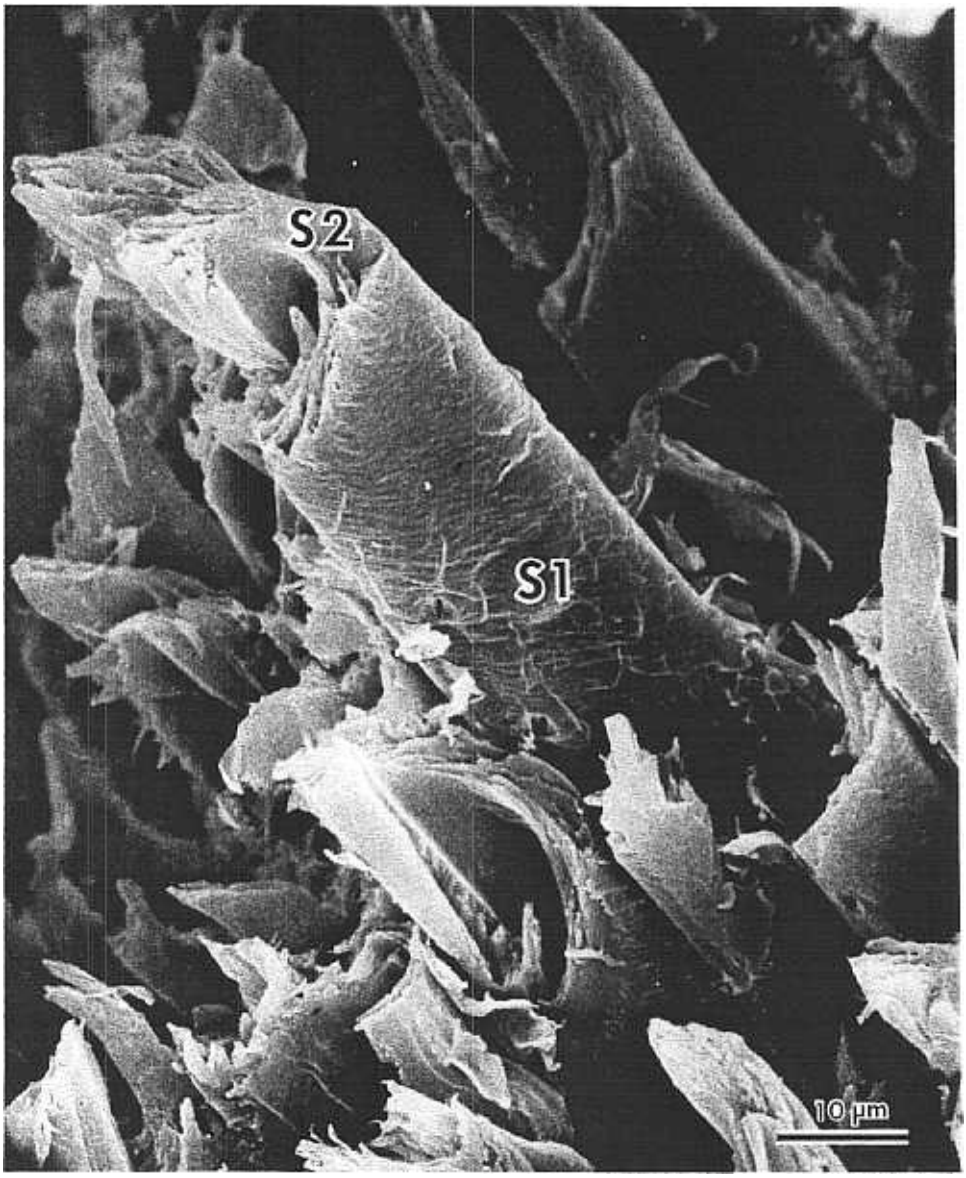

FIG. 18. In a wood of higher specific gravity such as red oak, tensile test specimens break with a less "brash" type of failure. Many individual fibers extend out of the failure zone. Clearly, intrawall failure predominates as S1 and S2 microfibrillar orientation can be seen throughout the micrograph.

ray A was the determining factor in the latewood, while ray B was the zone of weakness in the earlywood.

With respect to tangential shear, the failure plane generally was found in the earlywood region with the failures being transwall. In some cells, however, there was a separation at the S1/S2 interface which resulted in the S2-S3 layers peeling out (Fig. 16).

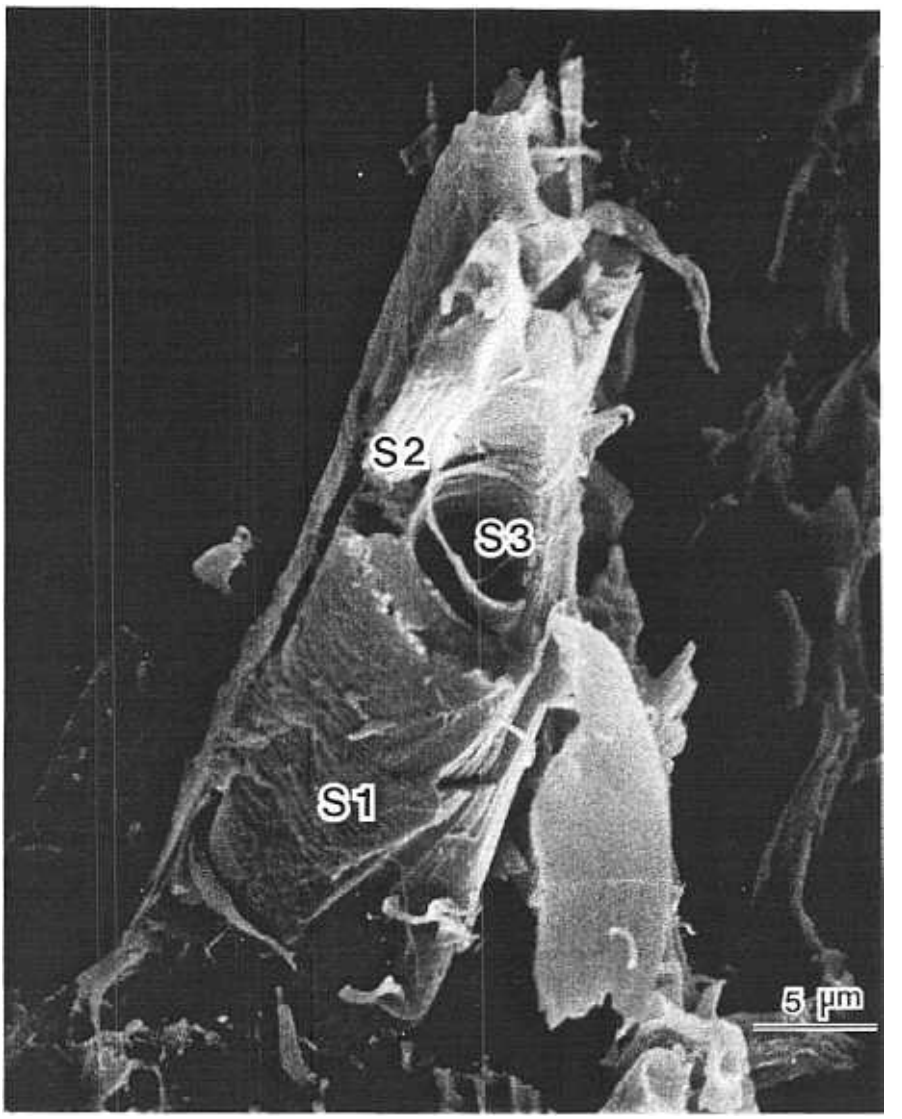

FIG. 19. These fibers in a tensile test specimen of hickory exhibit intrawall failure in which all three secondary wall layers can be identified through their orientation. Obviously transwall failure occurred ultimately as well.

Tension parallel to the grain

In hardwoods, tensile failure parallel to the grain resulted in an extremely complex fracture surface (Fig. 17). As a general rule tensile failure produced a transwall failure, which followed the S2 fibrillar angle in those cells having a thick S2 cell-wall layer. This "unwinding phenomenon" was probably the result of slippage between the microfibrils (Figs. 18, 19, 20). Also, within the same cells,

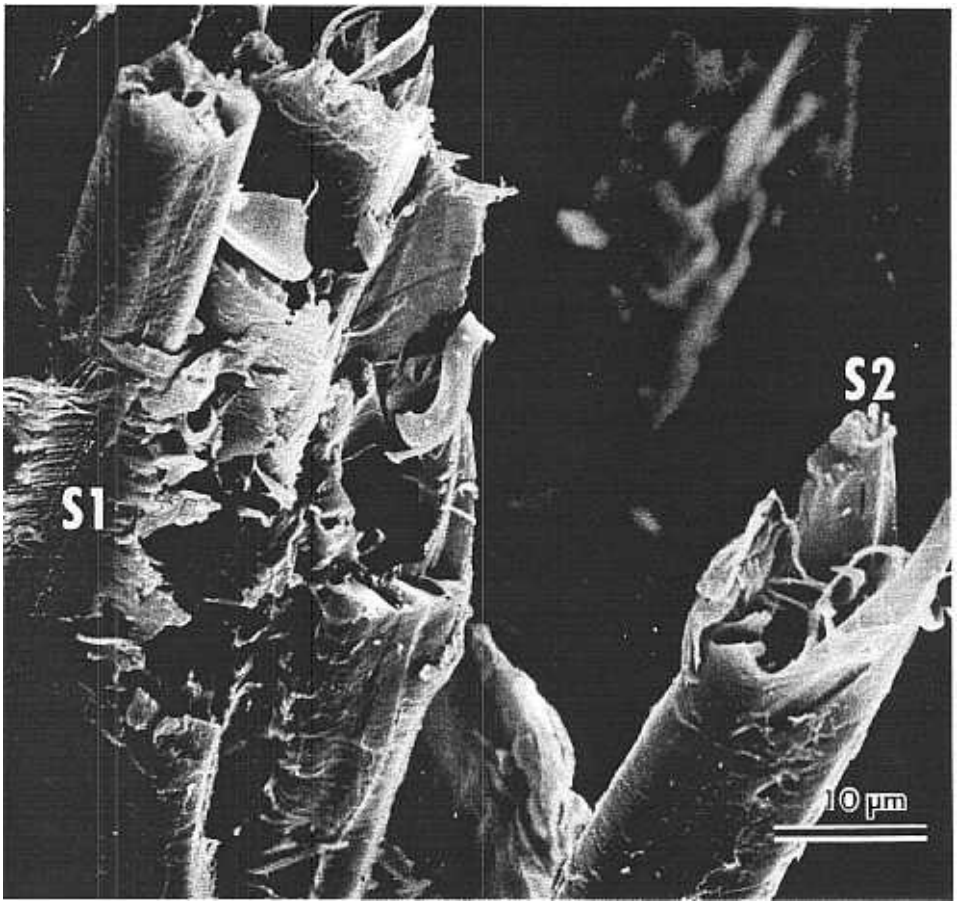

FIG. 20. The unwinding phenomenon discussed in the text appears in this specimen of hickory tested in tension parallel to the grain, as it has in several other instances. Intrawall failure at the S1/S2 predominates, while transwall failure is most evident at the S2 regions of the cell walls.

there was intrawall failure in the S1, which allowed the fiber core (S2 and S3) to pull out (Figs. 18, 19, 20). Conversely, in those cells with a diminished S2 cell-wall layer, the failure was of an abrupt transwall type (Fig. 21). There were, however, many instances where abrupt transwall failure was found in cells with a thick S2 (Fig. 20) and failures that had followed the S2 fibrillar angle were found in cells with a thin S2 (Fig. 17).

The failure patterns in softwood as represented by southern pine were surprisingly similar to the hardwoods. The thick-walled latewood tracheids failed with a transwall fracture, which followed the S2 microfibrillar orientation. This is illustrated in Fig. 22.

In earlywood tracheids that are thin-walled and punctuated by bordered pits, abrupt transwall fracture is typical. The relationship of the fracture zone to the location of bordered pit pairs in the compound cell walls was noted to be consistent. The stress concentrations invariably followed the edge or annulus region

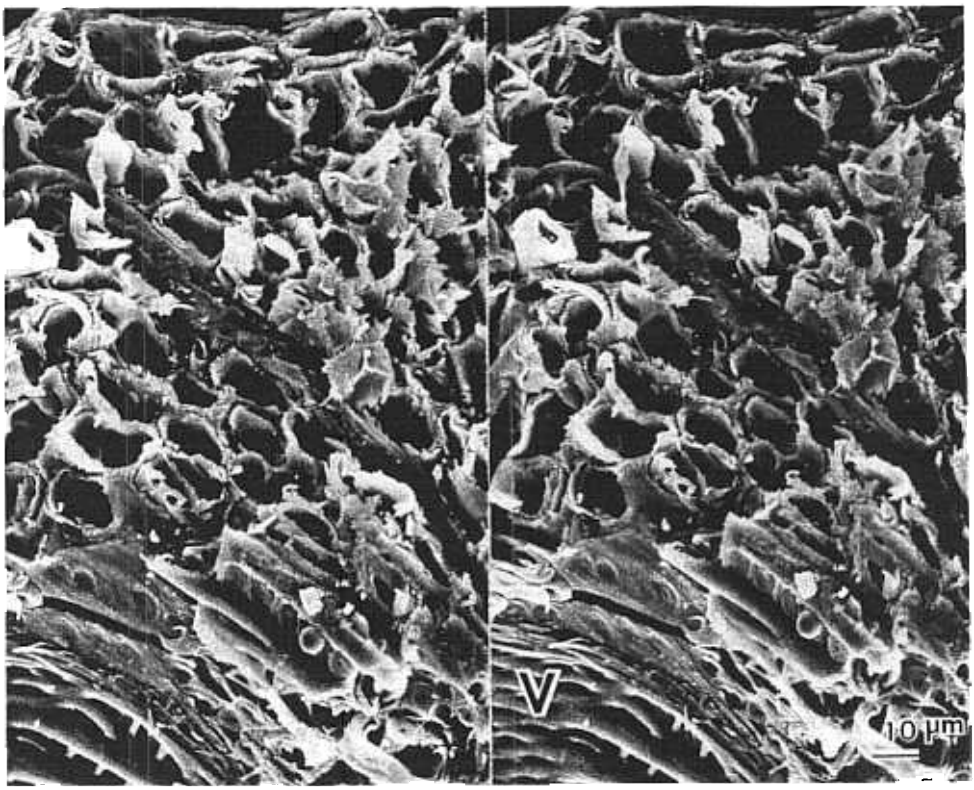

FIG. 21. In this stereo pair of a red oak tensile test specimen, an area from the earlywood has been selected to illustrate the abrupt transwall failure of the fibers as well as the vessel wall. Very few traces of long projections of cell wall can be found.

of the pit rather than traversing it. Several examples of this behavior can be seen in Fig. 23.

Thick-walled tracheids did fail in an abrupt transwall pattern in some instances such as in the area shown in Fig. 24. In other cases in latewood, the S2 layers pulled out of the S1 and then unwound as fracture proceeded. In Fig. 25, the unwinding phenomenon is more distinct than in the hardwoods because of the less sculptured wall structure of tracheids. Since virtually all of the longitudinally oriented elements are tracheids, the repetitive pattern of failure can be observed more readily.

CONCLUSIONS

The use of scanning microscopy to examine the anatomical and ultrastructural aspects of wood failure under mechanical test has been shown to be a valid and useful approach to a clearer understanding of the failure phenomena. A few general observations can be offered in summary of the findings detailed above. Also, suggestions are made for extension of this work in the future.

On the basis of the evidence presented and discussed in this report as well as on the large number of observations made in the course of this study, certain

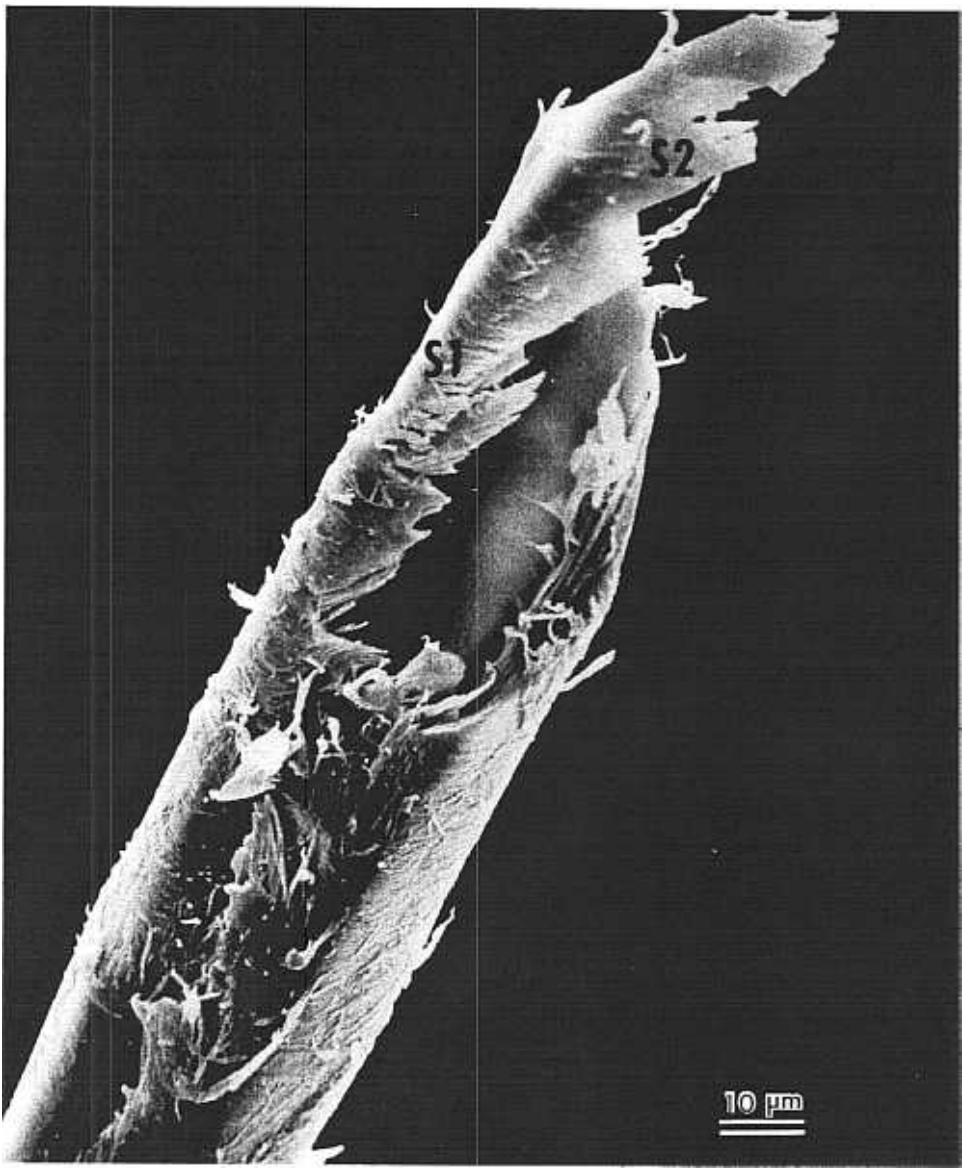

FIG. 22. This is an apparently unpitted portion of a southern pine latewood tracheid that failed in tension. The tendency of the S2 to unwind can be seen, while portions of the S1 with its nearly horizontal orientation of microfibrils remain.

characteristic types of failure can be related to each of the testing modes utilized. These have been considered in the discussion of each testing mode. Variation that occurs in each category appears to be determined by cell-wall thickness, both in hardwoods and in softwoods. Thick-wall cells tend to fail in an intrawall pattern at the S1/S2 interface, while thin-walled cells are more likely to fail with transwall fracture.

The variability of anatomy in hardwoods influences the nature of failure. For

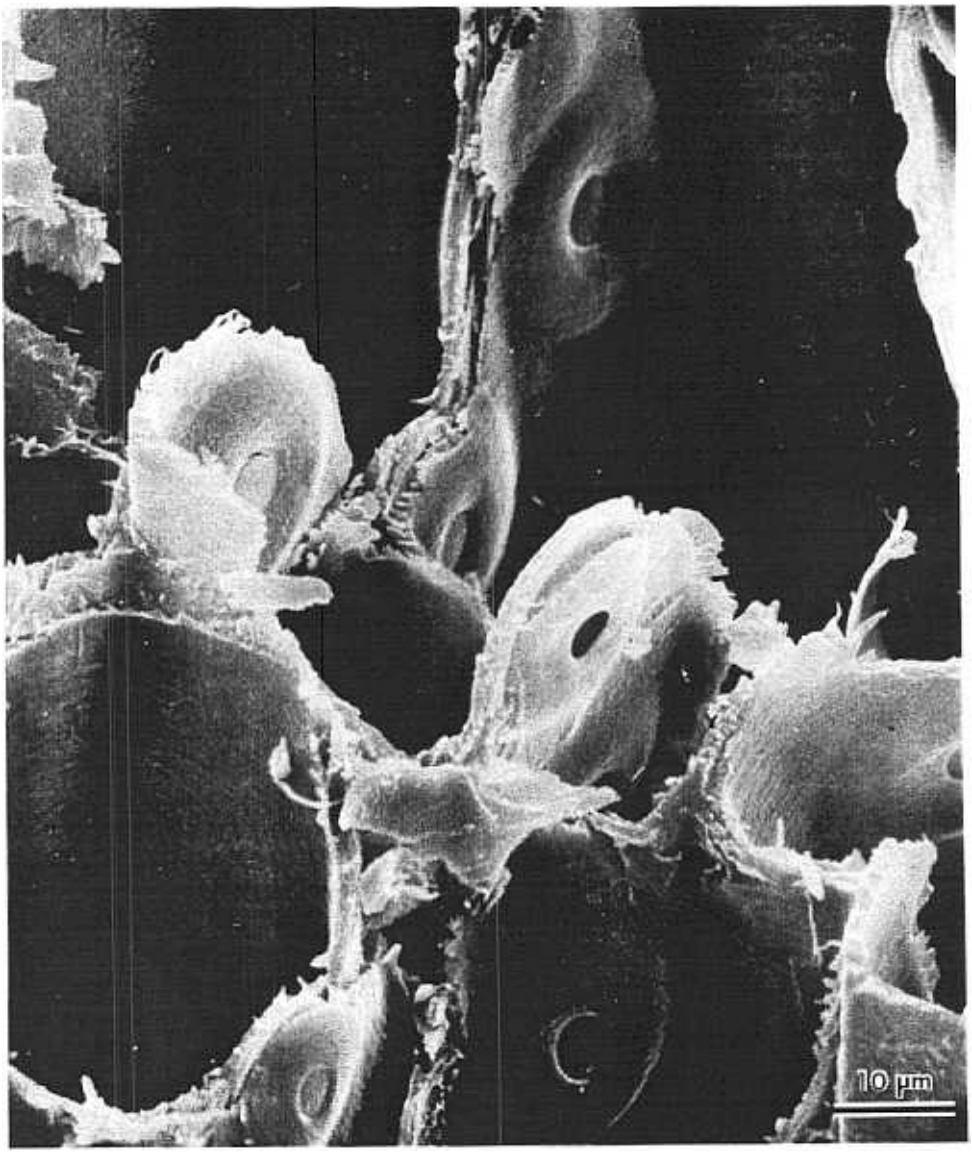

FIG. 23. Although much as been mentioned in the literature about the role of bordered pits in cell-wall failure in conifers, this is one of the few clear examples of their resistance to transwall failure. Instead, the fracture lines in these earlywood tracheids of southern pine follow the rim or annulus of the bordered pit pairs in several cases.

example, in tangential shear tests of ring-porous woods, the plane of fracture follows the earlywood vessels that are thin-walled and have wide lumens. The very large oak-type rays affect the fracture path in all the test modes. Normal rays have a major role in radial shear parallel to the grain since they represent a plane of weakness and step-wise failure results. However, even in compression parallel to the grain, the ray/longitudinal element interface represents a weak zone where intercell failure concentrates.

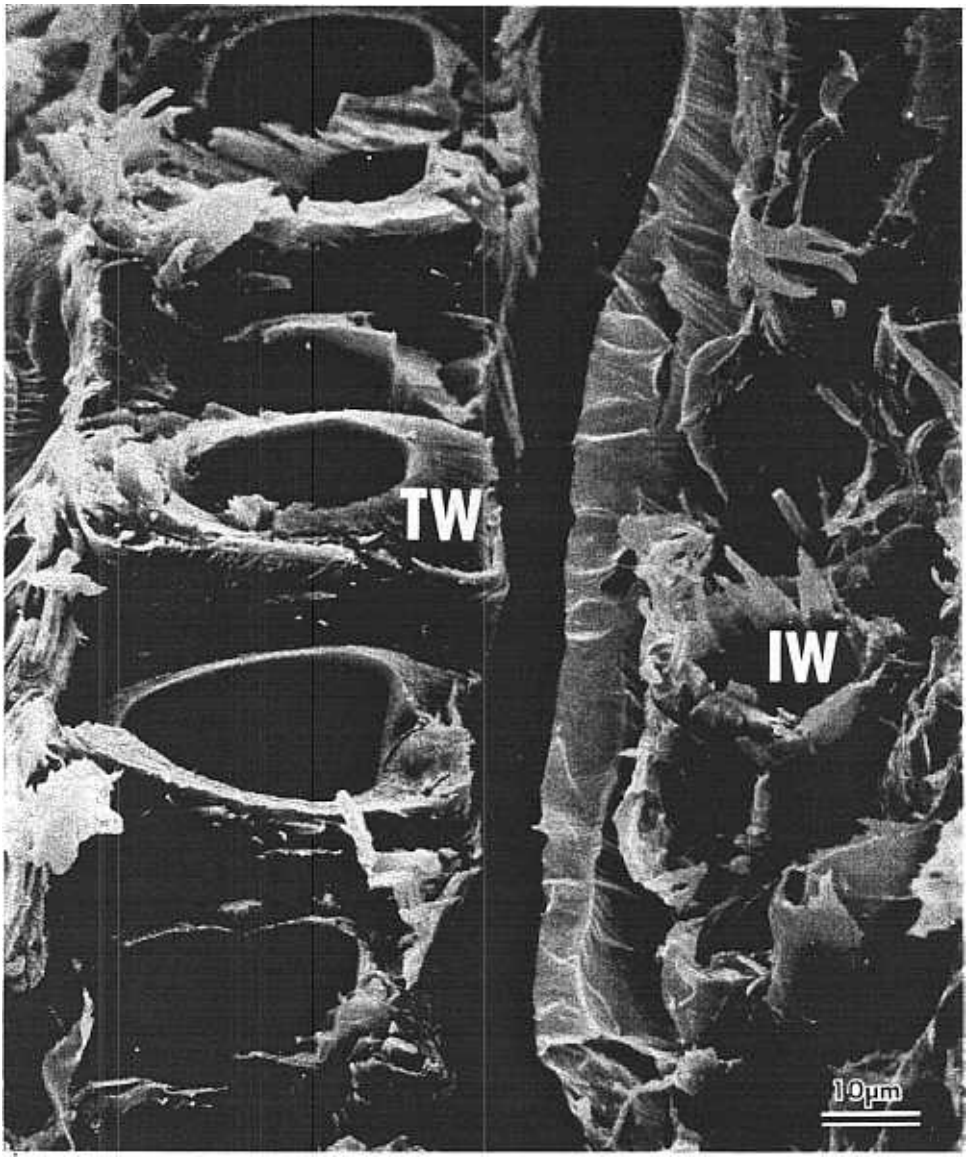

FIG. 24. On the left side of this micrograph, there is a row of thick-walled tracheids in the latewood of southern pine. All show abrupt transwall failure, while those on the other side of the ray that traverses the center of the micrograph from top to bottom exhibit more intrawall failure. It appears likely that the distribution of anatomical components influences tensile tests such as this just as it does in shear and compression tests.

It has not appeared possible to reconstruct the chronological order of events leading to ultimate failure from the evidence found in scanning electron micrographs. In the radial shear test specimens where step-wise failure goes from ray to ray along the grain, there is some suggestion of the direction of such events, however.

From the work of DeBaise et al. (1966) and DeBaise (1970), the rate of crack

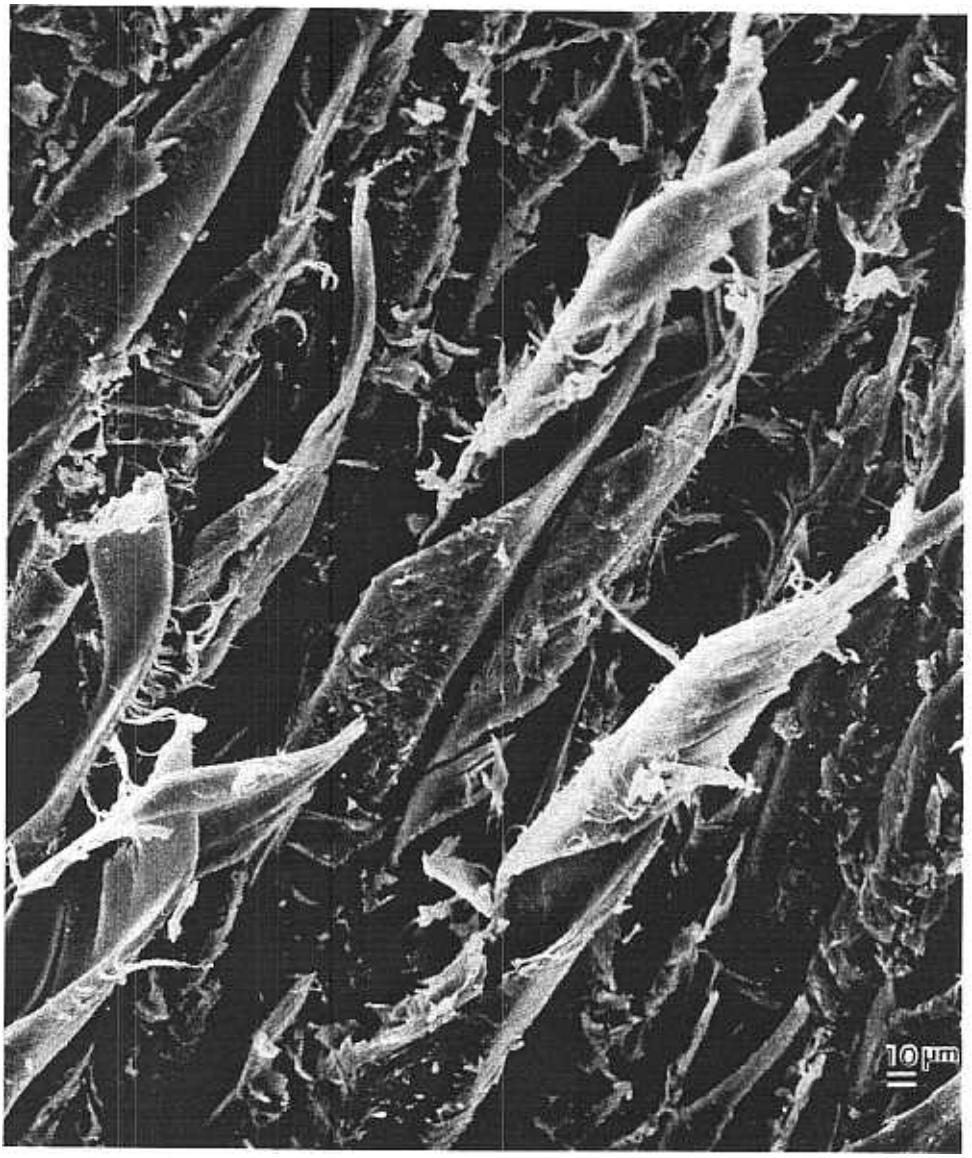

FIG. 25. In this example of southern pine latewood that failed in tension, evidently the S2 layers pulled out of the S1, which would presumably be found in the matching end of the test specimen. The unwinding phenomenon seen in both hardwoods and softwoods is found throughout this fracture surface and consists of S2 with only traces of the other layers.

propagation in tests of wood to failure was found to influence the nature of the fracture surface. In the work reported here, normal loading rates were used. It would be desirable to extend this research to samples produced at faster loading rates to compare the resulting fracture surfaces.

As suggested by the work of Kloot (1952) on micro-testing of wood, the preparation of even smaller test specimens for future research could lead to fruitful results. For example, the specimen could be limited to the earlywood or latewood

zone of a single growth ring. This would allow comparison of properties of samples taken from growth rings produced following certain silvicultural treatments. In adopting this approach, the increased probability and importance of artifact production during specimen preparation would require careful consideration as noted by Keith and Côté (1968).

ACKNOWLEDGMENTS

This study was initiated through the instigation of Dr. Peter Koch, U.S. Forest Service, Southern Forest Experiment Station, Pineville, Louisiana. We are grateful for the challenge he offered to characterize hardwood fracture ultrastructurally as well as for the support received.

We are indebted to several members of the research and support staff for their skilled assistance in carrying out various aspects of this work: Mr. Walter Maier of the Department of Wood Products Engineering for machining the test specimens and carrying out the test procedures; Miss Judy Barton of the same department for typing services; Mr. John J. McKeon of the N. C. Brown Center for Ultrastructure Studies for preparing a large number of photographic prints that were required during the study as well as in preparation of the final manuscript; and Mr. Arnold C. Day, also of the Center, who microtomed the specimens from the compression parallel to the grain tests.

REFERENCES

ASTM. 1976. Annual book of ASTM standards, Part 16, pp. 56–98. Tests for small clear specimens, D-143, Part II. Secondary methods. American Society for Testing Materials.

CLARKE, S. H. 1935. Forestry (London) 9:132.

DEBAISE, GEORGE R. 1970. Mechanics and morphology of wood shear fracture. Ph.D. dissertation, Dept. of Wood Products Engineering, State University College of Forestry at Syracuse University.

-. 1972. Morphology of wood shear fracture. J. Materials 7(4):568–572.

-, A. W. PORTER, AND R. E. PENTONEY. 1966. Morphology and mechanics of wood fracture. Mater. Res. Stand. 6(10):493–499.

KEITH, C. T., AND W. A. CÔTÉ. 1968. Microscopic characterization of slip lines and compression failures in wood cell walls. For. Prod. J. 18(3):67–74.

KLOOT, N. H. 1952. A micro-testing technique for wood. Aust. J. Appl. Sci. 3(2):125–143.

KOLLMANN, F. F. P. 1963. Phenomena of fracture in wood. Holzforschung 17(3):65–71.

KORAN, ZOLTAN. 1967. Electron microscopy of radial tracheid surfaces of black spruce separated by tensile failure at various temperatures. Tappi 50(2):60–67.

-. Undated. Electron microscopy of tangential tracheid surfaces of black spruce produced by tensile failure at various temperatures. Tech. Report No. 514, PPRIC, Canada.

TIEMANN, H. D. 1951. Wood technology, 3rd edition. Pitman Publ. Corp., New York.

WARDROP, A. B. 1951. Cell wall organization and the properties of the xylem. I. Cell wall organization and the variation of breaking load in tension of the xylem in conifer stems. Aust. J. Sci. Res., B 4(4):391–417.

———, AND F. W. ADDO-ASHONG. 1965. The anatomy and fine structure of wood in relation to its mechanical failure. Pages 169–199 *in* "Fracture"—The proceedings of the First Tewksbury Symposium, Univ. of Melbourne, Australia, 26–30 Aug. 1963.

WOODWARD, CLINTON. 1980. Fractured surfaces as indicators of cell wall behavior at elevated temperatures. Wood Sci. 13(2):83–86.